Critical Solution Behavior in a Binary Mixture of Gaussian Molecules. II

EUGENE HELFAND AND FRANK H. STILLINGER, JR.
Bell Telephone Laboratories, Incorporated, Murray Hill, New Jersey 07974

(Received 23 February 1968)

The critical solution properties of a model mixture have been examined. The system is composed of two gases (A and B) such that there are no AA or BB molecular interactions. The AB interaction is repulsive, with a negative Gaussian Mayer f function. The Mayer series for the free energy has been calculated through tenth power of the density (11-point graphs). By methods of Padé approximants nonclassical critical singularities have been found in the second composition derivative of the free energy (related to composition fluctuations), fourth composition derivative of the free energy, and the compressibility. An infinity in c_p and a cusp in c_v are inferred. Thermodynamic questions discussed are the relations among the properties with pressure, density, or temperature as the independent variable; and the scaling laws. The critical fluctuations are also examined from the point of view of correlation functions.

I. INTRODUCTION

In the past few years there has developed a focus of interest on the properties of systems in the neighborhood of their critical transition point. We have witnessed a significant advance in experimental studies, both from the point of view of improved standard techniques and the application of modern tools. Although theoreticians have not yet developed general means of penetrating the mystery of the critical singularities, important advances have been made. Thermodynamic inequalities have been proven, which limit the range of possible singular behavior. The scaling laws provide plausible relations among the various critical exponents. Finally, sophisticated means have been developed for extrapolating to the critical point series expressions for the thermodynamic and correlation functions. By far the greatest number of such studies have been based on high- or low-temperature expansions of properties of the Ising or Heisenberg models.

Recently the series method was also applied by us[1] to the study of the critical solution behavior of a fluid mixture. It was confirmed that the critical properties of this system show marked deviations from the classical (van der Waals) theory. In this paper we shall report on a refinement of the earlier quantitative results, and also survey the transition in mixtures more extensively.

The specific system under consideration has the qualitative features of real fluid mixtures, but a number of modelistic simplifications have been made to render the theory tractable.

In a mixture of A and B, with three pair potentials, $v_{AB}(r)$, $v_{AA}(r)$, and $v_{BB}(r)$, it is essential for a phase separation to occur that the interaction energy between unlike molecules be more repulsive than some sort of average of the AA and BB interaction energies. Since it is only necessary to construct the model so as to possess this relative energy relation, one may hope to retain the essential features of the phase transition, while affecting an enormous computational simplification, by regarding the pure fluids A and B as ideal:

$$v_{AA}=v_{BB}=0.$$

The series development of the properties of the system which has been employed is the Mayer series for the Helmholtz free energy as a function of density and composition. In order to evaluate the Mayer cluster integrals we have chosen the AB interaction to be such that the Mayer f function,

$$f(r)\equiv\exp[-\beta v_{AB}(r)]-1$$

is a negative Gaussian,[2]

$$f=-\exp(-r^2/a^2). \tag{1.1}$$

The model potential, v_{AB}, is purely repulsive, but retains the correct qualitative features of going to zero as $r\to\infty$ and becoming infinite as $r\to 0$.

We have determined the free-energy series through the tenth power of the density (11-point graphs). A study has been made of the second-order phase transition (phase separation) induced by increasing the pressure of the mixture at constant temperature and at the critical composition (for a discussion of varying temperature at fixed pressure see Sec. VI). Interest centers on three thermodynamic quantities. The second derivative of the free energy with respect to composition is a measure of composition fluctuations, hence it is like the inverse susceptibility of a magnet or compressibility of a pure fluid. The fourth derivative of free energy with respect to composition is related to a hypersusceptibility. The compressibility, which according to classical theories should be finite and greater than zero, has also been examined. Each of these properties appears to exhibit a nonclassical critical anomaly. The exponents characterizing these singularities have been estimated, primarily by Padé analysis. The scaling law (cf. Sec. II) relating the three properties has been found to be consistent with the data.

It is remarkably simple to study the properties of this system as a function of dimensionality, and even to construct a natural extension of the free-energy function for nonintegral dimension. In this way the quantitative and qualitative features of the disappear-

[1] F. H. Stillinger, Jr., and E. Helfand, J. Chem. Phys. **41**, 2495 (1964). The exponent γ of that paper is termed γ_p here.

[2] E. W. Montroll, T. H. Berlin, and R. W. Hart, *Changement de Phases* (Société de Chimie Physique, Presses Universitaires de France, Paris, 1952), p. 211.

This article is copyrighted as indicated in the article. Reuse of AIP content is subject to the terms at: http://scitation.aip.org/termsconditions. Downloaded to IP: 128.112.66.66 On: Sun, 29 Dec 2013 03:06:19

ance of the phase transition as the dimensionality is lowered have been traced (Sec. V).

From the information obtained about the singularities as a function of pressure at fixed temperature, the nature of the singularities as a function of temperature can be inferred (cf. Sec. VI). The specific heat at constant pressure is found to have the same type of singularity as the compressibility. The specific heat at constant volume has a cusp.

We also discuss the relation of the properties studied to the radial distribution functions and fluctuations near the critical point in Appendix A.

In Appendix B technical aspects of the generation of the Mayer graphs are presented.

II. PHENOMENOLOGY

A. Basic Thermodynamics[3]

A useful equation of state for characterization of the thermodynamic properties of binary mixtures is the Gibbs free energy as a function of pressure, composition, and temperature. For reasons inherent in the choice of potential the temperature is fixed and we consider changes which occur as the pressure is varied. When the system is quite dilute the intermolecular interactions are relatively unimportant and the entropy of mixing makes a dominant contribution to the free energy, rendering the mixture homogeneous. However as the system is compressed more particles interact in a typical configuration. If the interaction of unlike particles is more repulsive than the like-particle interactions the unmixing effect of the energy may dominate the homogenizing effect of the entropy, so that a phase transition occurs.

To understand the manner in which this is reflected in the free-energy curve, consider that one has, at a given pressure and temperature, two phases of different composition (separated by a wall if necessary). The Gibbs free energy per particle, $G/N \equiv g$, will lie along a line connecting the points corresponding to the two compositions in the g vs composition plane. Figure 1 is a plot of g vs x_A (mole fraction of A) for various pressures. Consider two separate phases with conditions c_1 and c_2. The free energy has a value somewhere along the tie line c_1c_2 and hence the homogeneous phase has lower free energy. Next consider c_3 and c_4. Coexisting phases of these compositions have a lower free energy than that of any other coexisting composition. The line c_3c_4 is the so-called double-tangent line. The slope of this line is $(\partial g/dx_A)_{p,T,N} = \mu_A - \mu_B$. Thus the fact that $\mu_A - \mu_B$ is a constant for all relative amounts of coexisting phases is exhibited. If, as a result of approximations in any statistical-mechanical calculation, one finds an unstable free-energy curve for some compositions, then

[3] Such a discussion was included in Ref. 1, but in this paper we will consider a wider range of phenomena. Furthermore, we take this opportunity to correct several errors (which, however, did not effect the previous results).

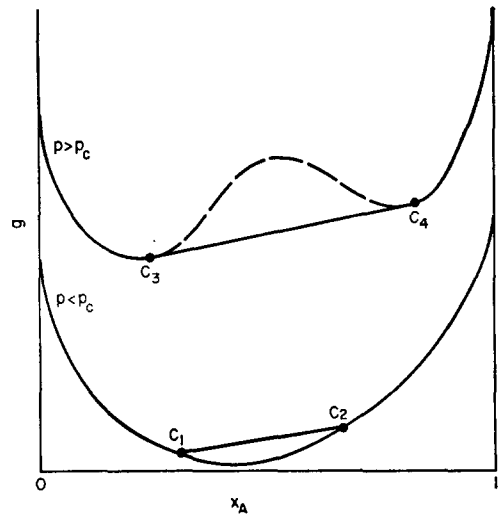

FIG. 1. Gibbs free energy vs composition. Tie lines represent free energies of separate phases. The low-pressure (lower) curve has all tie lines above. The segment c_3c_4 of the high-pressure (upper) curve represents the free energy of spontaneously coexistent phases.

the double-tangent construction may be used to determine the region in which coexisting phases are thermodynamically more stable. This is the case with the present calculation.

The critical pressure p_c divides those free-energy curves with a double-tangent region, from those with no double-tangent region. The borderline g curve possesses a single critical point at which $(\partial^2 g/\partial x_A^2)_p$ vanishes.

In the model we shall consider, a symmetry exists with respect to interchange of species A and B. This symmetry tends to simplify the thermodynamics; henceforth let us limit ourselves to a discussion of such symmetric situations. It is convenient to introduce a composition variable antisymmetric about the critical composition,

$$y = 2x_A - 1.$$

The Gibbs free energy $g(p, y)$ is symmetric in y so that the critical composition must be $y=0$. The equation for the critical pressure can be written in the special form

$$\chi^{-1}(p) \equiv [\partial^2 g(p, y=0)/\partial y^2]_p \tag{2.2}$$

$$\chi^{-1}(p_c) = 0. \tag{2.3}$$

By the notation we have indicated the relation of this second derivative to susceptibility; generally a susceptibility is the coefficient characterizing response to a force. In this case the response is composition, y, and the force is

$$-(\partial g/\partial y)_p \equiv -\tilde{\mu} = \tfrac{1}{2}(\mu_B - \mu_A).$$

(See Table I for a catalog of analogs to a magnet and to a pure fluid.) It is to be expected that as one ap-

This article is copyrighted as indicated in the article. Reuse of AIP content is subject to the terms at: http://scitation.aip.org/termsconditions. Downloaded to IP: 128.112.66.66 On: Sun, 29 Dec 2013 03:06:19

TABLE I. Thermodynamic analogies.

	Pure fluid	Magnet	Mixture[a]
Free energy	Helmholtz	$\mathfrak{F}(M, T)$	Gibbs, g
Force	p	H	$-\mu$
Response	V	$-M$	y
Susceptibility	$-(\partial V/\partial p)_T$	$(\partial M/\partial H)_T$	$(\partial y/\partial\tilde{\mu})_p$
Thermodynamic displacement	T	T	p
Conjugate force	S	S	$-1/\rho$
Specific-heat-like variable	c_V	c_M[b]	$(\partial\rho/\partial p)_y$

[a] For temperature-induced transition see Sec. VI.
[b] $c_H = c_M$ for $H=0$ and $T>T_c$.

proaches the critical point, χ diverges as

$$\chi(p) \propto (p_c-p)^{-\gamma}, \qquad p<p_c. \tag{2.4}$$

According to classical theory $\gamma=1$, but a nonclassical value greater than unity is found.

One suspects that this system will also exhibit other nonclassical critical-point characteristics. Magnets have a critical specific-heat singularity—the second derivative of the free energy with respect to the temperature diverges as the critical temperature is approached in zero field. For the model Gaussian mixture the transition is induced by varying the pressure rather than the temperature. Thus we expect (cf. Sec. VI) a specific-heat-like singularity in the compressibility, which is related to $(\partial^2 g/\partial p^2)_y = -\rho^{-2}(\partial\rho/\partial p)_y$. Near the critical point $(\partial\rho/\partial p)_{y=0}$ diverges like

$$(\partial\rho/\partial p)_{y=0} \propto (p_c-p)^{-\alpha}, \qquad p<p_c. \tag{2.5}$$

Another thermodynamic property which exhibits a critical singularity, and which is conveniently studied for the present model is $(\partial^4 g/\partial y^4)_p$. This quantity, related to hypersusceptibility, vanishes at the critical point like (definition of ϵ):

$$(\partial^4 g/\partial y^4)_p\,|_{y=0} \propto (p_c-p)^{\epsilon}, \qquad p<p_c. \tag{2.6}$$

B. Scaling Laws

In recent years an attempt has been made to provide a unifying thread among the critical singularities by means of the "scaling laws."[4] As applied to a symmetric mixture this theory states that the critical thermodynamic properties are embodied in a Gibbs free energy which has the functional form

$$g(p, y) = g_S(p, y) + g_N(p, y),$$
$$g_S(p, y) \sim |\, p_c-p \,|^{2-\alpha}\phi[(p_c-p)/|\, y \,|^{2/(2-\alpha-\gamma)}], \tag{2.7}$$

where g_S is the singular part of the Gibbs free energy.

[4] B. Widom, J. Chem. Phys. **43**, 3898 (1965); L. P. Kadanoff, Physics **2**, 263 (1966); A. Z. Patashinskii and V. L. Pokrovskii, Zh. Eksp. Teor. Fiz **50**, 439 (1966) [Sov. Phys—JETP **23**, 292 (1966)]; R. B. Griffiths, Phys. Rev. **158**, 176 (1967).

The essential behavior of the function $\phi(z)$ is fixed by a number of requirements. For $p<p_c$ the free energy is to be analytic and even in y. Thus, as $z\to\infty$, ϕ must have the form

$$\phi(z) \underset{z\to\infty}{\longrightarrow} a_0 + a_1 z^{-(2-\alpha-\gamma)} + a_2 z^{-2(2-\alpha-\gamma)} + \cdots, \tag{2.8}$$

or

$$g_S(p, y) \sim a_0(p_c-p)^{2-\alpha} + a_1(p_c-p)^{\gamma}y^2$$
$$+ a_2(p_c-p)^{2\gamma+\alpha-2}y^4 + a_3(p_c-p)^{3\gamma+2\alpha-4}y^6 + \cdots. \tag{2.9}$$

The first two terms reveal that the exponents α and γ employed in Eq. (2.7) are the same as those arising in the susceptibility, Eq. (2.4), and compressibility, Eq. (2.5). The third term predicts as a scaling law for ϵ

$$2\gamma+\alpha-\epsilon=2. \tag{2.10}$$

In most discussions of critical thermodynamics the exponent ϵ is not introduced; rather one employs the "gap exponent" Δ related to ϵ by

$$\epsilon = 3\gamma - 2\Delta.$$

[For a magnetic system Δ is defined from the hypersusceptibility as

$$(\partial^4 F/\partial H^4)_T\,|_{H=0} \propto (T-T_c)^{-\gamma-2\Delta}. \tag{2.11}]$$

For the Gaussian mixture we have numerically estimated only α, γ, and ϵ. There are several other critical properties of interest. Along the critical isobar, $p=p_c$, the chemical potential difference $\tilde{\mu}$ is related to composition by

$$|\,\tilde{\mu}\,| \propto |\, y \,|^{\delta}. \tag{2.12}$$

If the free energy (2.7) is to represent a function which is analytic in $p-p_c$ for nonzero y, then for small z, ϕ must have the form

$$\phi(z) \underset{z\to 0}{\longrightarrow} |\, z \,|^{\alpha-2}[b_0 + b_1 z + b_2 z^2 + \cdots];$$

so that

$$g_S(p, y) \sim b_0 |\, y \,|^{2(2-\alpha)/(2-\alpha-\gamma)}$$
$$+ b_1 |\, y \,|^{2(1-\alpha)/(2-\alpha-\gamma)}(p_c-p) + \cdots. \tag{2.13}$$

The scaling law for δ which results is

$$\delta = (2-\alpha+\gamma)/(2-\alpha-\gamma). \tag{2.14}$$

For $p>p_c$ the two coexisting phases are characterized by a coexisting composition, y_{coex}, which vanishes at the critical point like

$$y_{\text{coex}} \propto (p-p_c)^{\beta}. \tag{2.15}$$

At this coexistent composition the chemical potential $\tilde{\mu}$ must vanish, but the susceptibility is finite. Thus the function ϕ must go to zero at some point, $-k$, like

$$\phi(z) \underset{z\to -k+}{\longrightarrow} c(z+k)^2. \tag{2.16}$$

This article is copyrighted as indicated in the article. Reuse of AIP content is subject to the terms at: http://scitation.aip.org/termsconditions. Downloaded to IP: 128.112.66.66 On: Sun, 29 Dec 2013 03:06:19

The equation for the coexistence curve is $z+k=0$, which implies the scaling law

$$\alpha+2\beta+\gamma=2. \tag{2.17}$$

The susceptibility and compressibility along the coexistence curve can be shown to diverge like $\chi \propto (p-p_c)^{-\gamma'}$ and $(\partial\rho/\partial p)_{\tilde{\mu}} \propto (p-p_c)^{-\alpha'}$ with $\gamma'=\gamma$ and $\alpha'=\alpha$.

C. Density as an Independent Variable

The Mayer theory, which we have applied to the study of the Gaussian mixture, yields directly the Helmholtz free energy per particle f as a function of density ρ and composition y. The previous discussion was in terms of the Gibbs free energy because with pressure as the independent variable closer analogy to the usual discussions of critical phenomena can be made. The information contained in one free-energy function or the other is interconvertible. There are two options, both of which we have pursued. One can convert the series for $f(\rho, y)$ to a series for $g(p, y)$ by means of a Legendre transformation; or one can analyze the critical singularities in ρ, y variables and relate the observed singularities to those in p, y variables. The thermodynamics of the latter approach will now be discussed.

A basic relation for this analysis arises from integration of the compressibility in the neighborhood of the critical point. For $y=0$:

$$\rho_c-\rho=\int_p^{p_c}\left(\frac{\partial\rho}{\partial p}\right)_y dp,$$
$$\propto (p_c-p)^{1-\alpha}, \qquad p<p_c. \tag{2.18}$$

Consider, now, the relation between composition derivatives of the Helmholtz and Gibbs free energies:

$$f=g+p/\rho, \tag{2.19}$$

$$(\partial f/\partial y)_\rho=\tilde{\mu}=(\partial g/\partial y)_p, \tag{2.20}$$

$$(\partial^2 f/\partial y^2)_\rho=(\partial^2 g/\partial y^2)_p+(\partial\tilde{\mu}/\partial p)_y(\partial p/\partial y)_\rho. \tag{2.21}$$

By symmetry $(\partial\tilde{\mu}/\partial p)_y$ and $(\partial p/\partial y)_\rho$ vanish for $y=0$. Thus by Eqs. (2.4), (2.18), and (2.21), and $\rho>\rho_c$,

$$\chi^{-1}(\rho)=(\partial^2 f/\partial y^2)_\rho \propto (\rho-\rho_c)^{\gamma/(1-\alpha)}. \tag{2.22}$$

If we write

$$\chi(\rho) \propto (\rho-\rho_c)^{\gamma_\rho}, \tag{2.23}$$

then

$$\gamma_\rho=\gamma/(1-\alpha). \tag{2.24}$$

Differentiating further we find

$$(\partial^4 f/\partial y^4)_\rho\,|_{y=0}=(\partial^4 g/\partial y^4)_\rho\,|_{y=0}+O(p_c-p)^{2\gamma-2+\alpha};$$
$$\sim(\rho_c-\rho)^{\epsilon_\rho}; \tag{2.25}$$

Thus

$$\epsilon_\rho=\min\{[\epsilon/(1-\alpha)], [(2\gamma-2+\alpha)/(1-\alpha)]\}. \tag{2.26}$$

According to scaling laws the two quantities in parentheses are equal.

Finally we have

$$[(\partial/\partial\rho)\rho^2(\partial f/\partial\rho)]_y=(\partial p/\partial\rho)_y$$
$$=-\rho^{-2}(\partial^2 g/\partial p^2)_y^{-1}$$
$$=(\rho_c-\rho)^{\alpha_\rho}, \tag{2.27}$$

$$\alpha_\rho=-\alpha/(1-\alpha),$$
$$\alpha=-\alpha_\rho/(1-\alpha_\rho). \tag{2.28}$$

Note that α_ρ is negative as defined here, but with this definition the scaling laws are the same for the density or pressure exponents.

A scaling law which will be tested in Sec. IV is [cf. Eq. (2.10)]

$$t\equiv 2\gamma_\rho+\alpha_\rho-\epsilon_\rho=2. \tag{2.29}$$

The characteristic factor $1/(1-\alpha)$ or $1/(1-\alpha_\rho)$ involved in transformation of the exponents from those appropriate to one set of variables to another is analogous to the same factor which has arisen in the development of the Syozi model of a dilute ferromagnet[5] or Widom's mixture analysis.[6]

III. THE GAUSSIAN MIXTURE MODEL

The mixture under consideration consists of two ideal gases which have a repulsive potential between unlike species, such that at some temperature the Mayer f is given by $-\exp(-r^2/a^2)$. This model has the following features, described more fully in Ref. 1. The only nonvanishing Mayer integrals correspond to bicolored graphs (cf. Appendix B). The Mayer integral corresponding to a graph G composed of p vertices and b bonds is given in d dimensions by

$$V^{-1}\int d\mathbf{r}_1\cdots d\mathbf{r}_p \prod_G f(r_{ij})=(-1)^b(\pi a^2)^{(p-1)d/2}D_G^{-d/2}. \tag{3.1}$$

D_G, the graph complexity, is evaluated as follows. Build a $p\times p$ matrix with -1 in the ij position if the graph has a bond connecting i and j, and zero otherwise. In the ii position put the number of bonds entering vertex i. Strike out any row and the corresponding column. The resulting determinant is D_G.

The free-energy function is composed of an ideal part plus a series wherein Mayer integrals corresponding to the set $\mathcal{G}_{n_A,n_B}$ of irreducible bicolored graphs of n_A type-A vertices and n_B type-B vertices contribute to the coefficient of

$$\rho^{n_A+n_B-1}x_A^{n_A}x_B^{n_B}.$$

[5] I. Syozi, Progr. Theoret. Phys. (Kyoto) **34**, 189 (1965); J. W. Essam and H. Garelick, Proc. Phys. Soc. (London) **92**, 136 (1967).

[6] B. Widom, J. Chem. Phys. **46**, 3324 (1967).

This article is copyrighted as indicated in the article. Reuse of AIP content is subject to the terms at: http://scitation.aip.org/termsconditions. Downloaded to IP: 128.112.66.66 On: Sun, 29 Dec 2013 03:06:19

TABLE II. The coefficients C_{nm} and number of graphs.

n	m	$C_{nm}\times 10^k$	k	No. of graphs
1	1	−1.0	0	1
2	2	3.125	2	1
2	3	2.00469	3	1
2	4	1.15089	4	1
3	3	3.85290	3	4
2	5	5.82309	6	1
3	4	9.50321	4	7
2	6	2.61027	7	1
3	5	1.45696	4	12
4	4	4.08055	4	29
2	7	1.04622	8	1
3	6	1.72075	5	18
4	5	2.53870	4	127
2	8	3.78442	10	1
3	7	1.69453	6	26
4	6	8.17069	5	361
5	5	5.65113	5	568
2	9	1.24590	11	1
3	8	1.44927	7	35
4	7	1.78289	5	892
5	6	4.42854	5	5714

Explicitly,

$$\frac{f}{kT}=\sum_{i=A,B}\left[\tfrac{3}{2}x_i\log\left(\frac{h^2}{2\pi m_i kT}\right)+x_i\log x_i\right]-\log(\pi^{d/2}a^d e)$$
$$+\log\rho-\sum_{n_A,n_B\geq 0}\rho^{n_A+n_B-1}\left[\tfrac{1}{2}(1+y)\right]^{n_A}\left[\tfrac{1}{2}(1-y)\right]^{n_B}C_{n_A n_B}, \tag{3.2}$$

where ρ is a reduced density given by

$$\rho=(N/V)\pi^{d/2}a^d. \tag{3.3}$$

The coefficients, $C_{nm}(=C_{nm})$ are given in Table II.

The reduced pressure will be selected as

$$p=\rho^2(\partial f/\partial\rho)_y,$$
$$=\pi^{d/2}a^d(N/V)^2\left[\partial f/\partial(N/V)\right]_y,$$
$$q=p/kT. \tag{3.4}$$

IV. ANALYSIS OF CRITICAL-POINT EXPONENTS

A. Method of Analysis

From the Helmholtz free energy one may derive density series expansions for thermodynamic functions such as susceptibility, hypersusceptibility, and compressibility which exhibit critical point anomalies of the type $(\rho_c-\rho)^{-\theta}$ for $y=0$.

One method of analyzing for such divergences is the ratio test. A series

$$f(x)=\sum b_n x^n, \tag{4.1}$$

which represents a function with closest singularity to the origin of type $(x_c-x)^{-\theta}$ may be studied by plotting $|b_n/b_{n-1}|$ vs $1/n$. In the limit of small $1/n$ the plot should be linear with intercept $1/x_c$ and slope $(\theta-1)/x_c$.

A somewhat more systematic approach to the problem, which in many cases also gives superior results, is analysis by Padé approximants[7]; i.e., fitting a function by the ratio of two polynomials $P_m(x)/Q_n(x)$ [called the (n, m) Padé approximant]. Baker, Gilbert, Eve, and Rushbrooke[8] suggested four ways in which functions $f(x)$ with singularities of the type $(x_c-x)^{-\theta}$ may be analyzed.

(i) Fit the logarithmic derivative of the function, $d\log f/dx$, which has a simple pole at x_c with residue θ.

(ii) Assume x_c is known and evaluate the Padé approximants to $(x-x_c)d\log f/dx$ at x_c to determine θ.

(iii) Assume θ is known and evaluate the Padé approximants to $[f(x)]^{1/\theta}$ to locate the pole x_c.

(iv) Examine

$$\frac{d\log f}{dx}\Big/\frac{d}{dx}\left(\log\frac{d}{dx}\log f\right)$$

which at x_c has the value θ. It is found that this function is usually only weakly dependent on x near x_c, so x_c need not be known too accurately.

To this list may be added (v).

(v) Examine

$$\frac{d}{dx}\left(\log\frac{d}{dx}\log f\right)$$

which should have a pole at x_c with residue one. If need be, use method (ii) to find the x_c which gives a residue of one.

The difficulty with methods (i), (iv), and (v) in the application discussed in this paper is that different choices of m and n yield somewhat scattered values for the exponent θ. Less scatter has been observed for methods (ii) and (iii) but no independent technique exists for selecting either θ or x_c. Practical aspects of the application of these techniques will emerge in the discussion of specific cases.

B. Susceptibility

$$kT\chi(\rho)=1.0+0.5\rho+0.25\rho^2+0.11719\rho^3+0.054186\rho^4$$
$$+0.024521\rho^5+0.010947\rho^6+0.0048374\rho^7$$
$$+0.0021180\rho^8+0.00092103\rho^9+0.00039816\rho^{10}+\cdots. \tag{4.2}$$

Plots of the ratio of successive coefficients of the series for $\chi(\rho)$ exhibit a bit too much curvature for points down to $n=10$ for effective application of the ratio test. A more incisive ratio test is a plot of the ratio $r_n(\gamma^*)$ of successive coefficients of $[\chi(\rho)]^{1/\gamma^*}$ vs

[7] G. A. Baker, Jr., Advan. Theoret. Phys. 1, 1 (1965).
[8] G. A. Baker, H. E. Gilbert, J. Eve, and G. S. Rushbrooke, Phys. Letters 20, 146 (1966).

This article is copyrighted as indicated in the article. Reuse of AIP content is subject to the terms at: http://scitation.aip.org/termsconditions. Downloaded to IP: 128.112.66.66 On: Sun, 29 Dec 2013 03:06:19

$1/n$ (Fig. 2). The value of γ^* yielding the closest approach to a horizontal line is selected as γ_ρ. On this basis we estimate that γ_ρ is between 1.68 and 1.76. The intercept is $1/\rho_c$, but the choice of this intercept is clearly dependent on which γ^* one selects as γ_ρ. A plot of this γ_ρ, ρ_c relation is contained in Fig. 3.

Padé approximants to the logarithmic derivative of $\chi(\rho)$ also exhibit some scatter in the prediction of γ_ρ and ρ_c for various (n, m). A similar γ_ρ vs ρ_c relation is exhibited however. The results of some pertinent Padés are included also in Fig. 3.

A common feature of these approximants to the logarithmic derivative of $\chi(\rho)$ is a tendency to have four poles and two zeros, as illustrated schematically in Fig. 4. With the length of series now available one

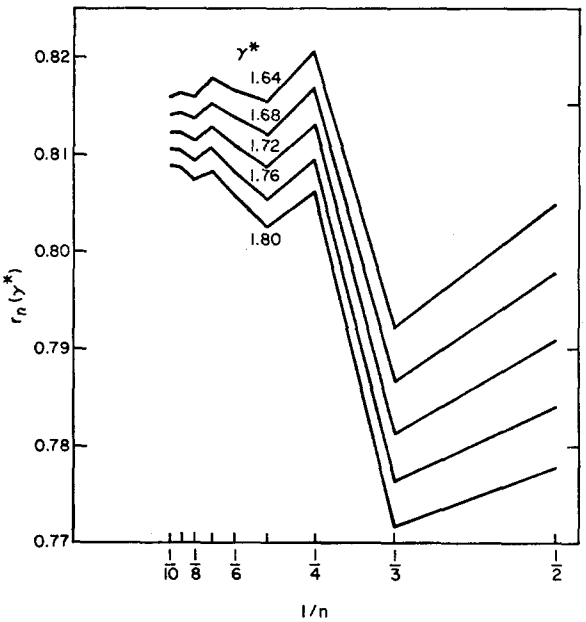

FIG. 2. The ratio, $r_n(\gamma^*)$, of the coefficients of the nth to the $(n-1)$th term of χ^{1/γ^*}.

can fit three more poles or zeros. The position of these is not clearly indicated by the present work and one may conjecture that the next feature which the Padés are trying to fit is a pair of complex poles with nearby zeros. Thus convergence in the Padé table may be in steps of four terms.

Padé analysis of $(\rho-\rho_c)d\ \log\chi/d\rho$ and χ^{1/γ_ρ} also reveals a close relationship between the choices of ρ_c and the prediction of γ_ρ (Fig. 2). One finds that if one has γ_ρ very far from 1.72 or ρ_c very far from 2.463 the various Padés begin to differ somewhat in their predictions, but otherwise there is little indication of how to select a γ_ρ, ρ_c pair.

The function

$$(d\ \log\chi/d\rho)/(d/d\rho)\ \log(d/d\rho)\ \log\chi$$

should be regular at ρ_c with value γ_ρ [method (iv)].

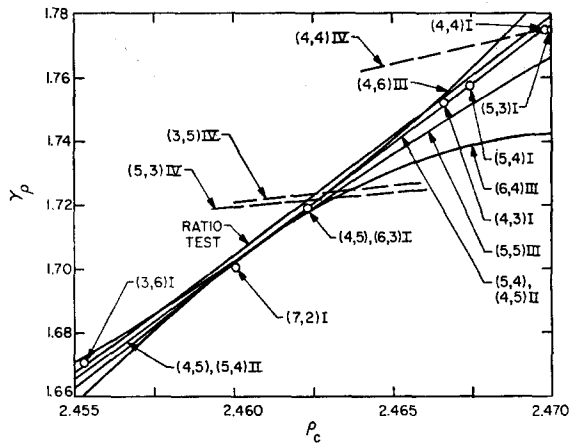

FIG. 3. A sampling of the results of Padé analysis and ratio test applied to the susceptibility series. Plotted is the prediction of γ_ρ and ρ_c by various methods (denoted by roman numerals). Numbers in parentheses indicate order of approximant.

Padé approximants to this function yield a value only slightly dependent on the choice of ρ_c as indicated in Fig. 2. However, the γ_ρ prediction varies somewhat with the choice of (n, m).

There is no systematic method of selecting γ_ρ and ρ_c from the foregoing analysis. Most of the evidence centers on a value of γ_ρ of 1.72 and $\rho_c=2.463$. These values will be selected as a basis for further discussion. A subjective error guess (50% feeling of confidence) for γ_ρ might be ± 0.03 with the possibility of a much greater error due to unexpectedly slow convergence. One should not think of these errors estimated in terms of Gaussian error curves.

C. Compressibility

$$[kTK(\rho)]^{-1}=1.0+0.5\rho-0.023438\rho^3-0.0025059\rho^4$$
$$-0.0019139\rho^5-0.00062747\rho^6-0.00015312\rho^7$$
$$-0.000076244\rho^8-0.000019627\rho^9-0.0000066880\rho^{10}$$
$$+\cdots. \quad (4.3)$$

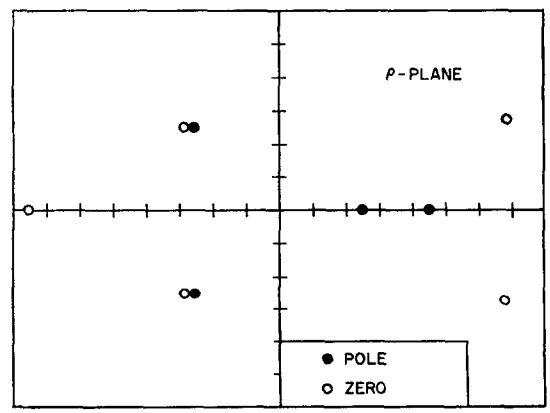

FIG. 4. Location of poles and zeros of the (4, 5) approximant to $d\ \ln\chi/d\rho$. The four poles and two zeros closest to the origin seem to be real features with only slight variation for different (n, m); the others vary unsystematically.

This article is copyrighted as indicated in the article. Reuse of AIP content is subject to the terms at: http://scitation.aip.org/termsconditions. Downloaded to IP: 128.112.66.66 On: Sun, 29 Dec 2013 03:06:19

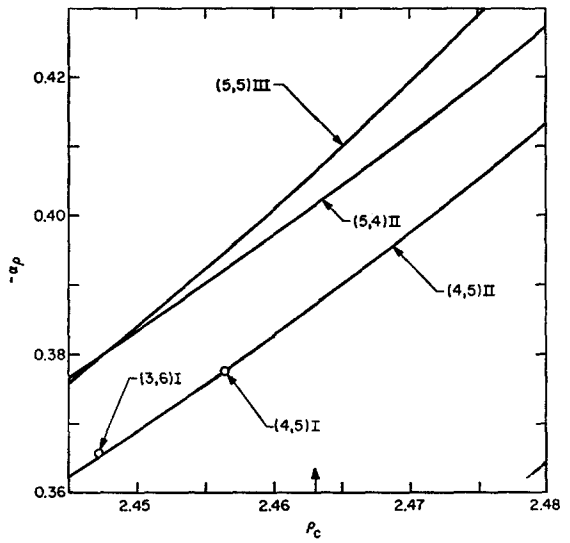

FIG. 5. A sampling of the results of Padé analysis applied to the compressibility series. The arrow at $\rho_c=2.463$ indicates the value selected from the susceptibility analysis.

The singularity in $K(\rho)\equiv\partial\rho/\partial p\,|_{y=0}$ is not as clearly determined as is the case for the susceptibility. This parallels the situation which exists for the analogous quantities in lattice models. One can, however, establish a fairly decent relation between the best choices of α_ρ and ρ_c. Selecting $\rho_c=2.463$ from the susceptibility analysis yields $\alpha_\rho=-0.40$. An estimate of the latitude in this choice of α_ρ would be about ±0.03.

These results are based on Padé analysis as summarized in Fig. 5. Many of the method (i) predictions fall off the graph, but not in any consistent pattern. The difficulty is probably associated with the fact that the dominant feature of $\partial\log K/\partial\rho$, which is reproducibly fit, is a zero near $\rho=1.72$ (between 0 and ρ_c). A pole near $\rho=2.4$ is present but not firmly located. The α_ρ's of method (iv) are mostly higher than -0.4, closer to -0.1. These are not too reliable since

$$\frac{d}{d\rho}\log\frac{d}{d\rho}\log K$$

does not clearly exhibit a pole near ρ_c.

D. Hypersusceptibility

$$f^{(4)}(\rho)/kT\equiv(\partial^4 f/\partial y^4)_\rho\,|_{y=0}/kT$$
$$=2.0-0.046875\rho^3-0.0030070\rho^4$$
$$-0.0042482\rho^5-0.0010582\rho^6$$
$$-0.00022904\rho^7-0.00013311\rho^8$$
$$-0.000019793\rho^9-0.0000077975\rho^{10}-\cdots. \quad (4.4)$$

In this section we consider the analysis of the density series for $f^{(4)}$ under the assumption that the singularity is of the form $(\rho_c-\rho)^{\epsilon_\rho}$. The nonideal contributions to $f^{(4)}$ begin with ρ^3 so that effectively the series is shorter than those for χ or K.

The logarithmic derivative Padés tend to scatter in their prediction of ϵ_ρ and ρ_c. Methods (ii) and (iii) are fairly effective in determining ϵ_ρ if ρ_c is taken as 2.463. The data are summarized in Fig. 6. A value of $\epsilon_\rho=1.00$ with uncertainty of ±0.05 is reasonable.

The indication of methods (i), (iv), and (v) is that the singularity is somewhat higher than $\rho=2.463$; probably this is a sign of slow convergence.

E. Susceptibility (Pressure Variable)

$$kT\chi(q)=1.0+0.5q+0.125q^2+0.054687q^3$$
$$+0.0082879q^4+0.0076947q^5-0.0010219q^6$$
$$+0.0019561q^7-0.00099292q^8+0.00083107q^9$$
$$-0.00057263q^{10}+\cdots. \quad (4.5)$$

Analysis of the susceptibility series (also the compressibility and hypersusceptibility) reveals that there is a singularity (perhaps a branch point) on the negative q axis closer to the origin than q_c. Generally, the Padé poles and zeros, other than the critical one, are devoted to fitting this feature.

Figure 7 illustrates some of the results of Padé analysis. Off the graph are the following method (i) results: from the (5, 4), $q_c=3.461$, $\gamma=1.332$; from the (3, 6), $q_c=3.456$ and $\gamma=1.280$. These are apparently isolated results, but their existence should not be forgotten. Also not shown in Fig. 7 are the results of method (v), which indicate q_c between 3.427 and 3.432.

We have selected the values $\gamma=1.22$, $q_c=3.430$, with a subjective uncertainty (50% confidence feeling) of ±0.05 in γ. This is to be contrasted with the thermodynamic relation $\gamma_\rho/(1-\alpha_\rho)=1.23$.

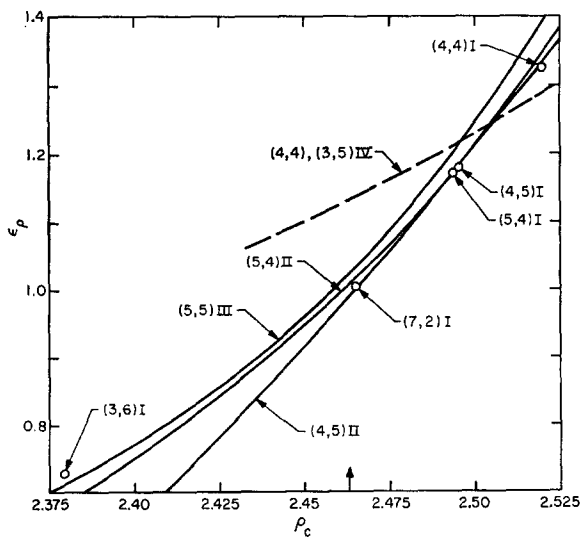

FIG. 6. Analysis of $f^{(4)}$. Note the greatly compressed scale, and the indications that ρ_c is greater than 2.463.

This article is copyrighted as indicated in the article. Reuse of AIP content is subject to the terms at: http://scitation.aip.org/termsconditions. Downloaded to IP: 128.112.66.66 On: Sun, 29 Dec 2013 03:06:19

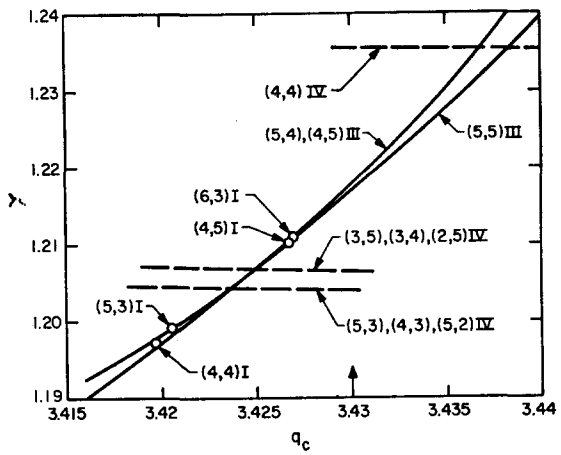

FIG. 7. A sampling of results of Padé analysis applied to the susceptibility as a function of pressure.

F. Compressibility (Pressure Variable)

$$kTK(q) = 1.0 - 0.5q + 0.375q^2 - 0.28906q^3 + 0.23200q^4 - 0.18792q^5 + 0.15370q^6 - 0.12633q^7 + 0.10425q^8 - 0.086273q^9 + 0.071548q^{10} + \cdots. \quad (4.6)$$

Again there appear to be singularities closer to the origin than q_c, although not on the real, positive axis. Only methods (ii) or (iii) which fix q_c or α yield results of interest (i.e., show a consistent pattern). Taking $q_c = 3.430$ one finds from the data displayed in Fig. 8 that $\alpha = 0.24 \pm 0.02$. The uncertainty associated with the failure of methods (iv) and (v) and the spread of (i) is difficult to appraise.

The value $\alpha = 0.24$ is significantly lower than that given by $\alpha = -\alpha_\rho/(1-\alpha_\rho) = 0.29$. Thus the difficulties

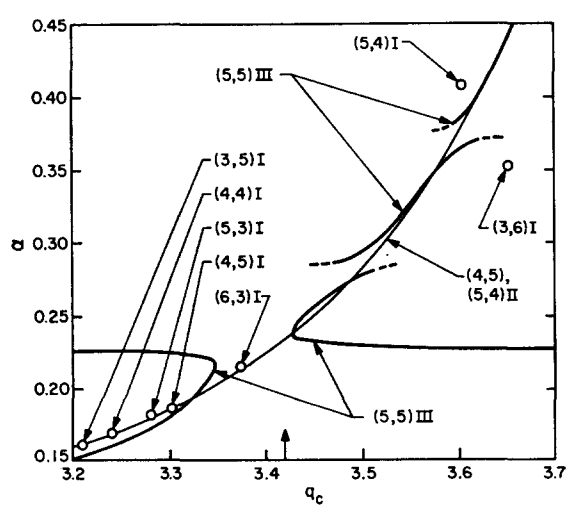

FIG. 8. Analysis of the compressibility in pressure variables. The scale is greatly compressed over Fig. 7 to include the method (i) results. The q_c selected from susceptibility considerations is indicated by an arrow. The (5, 5) (iii) curve exhibits the type of peculiar results which sometimes emerge from Padé analysis.

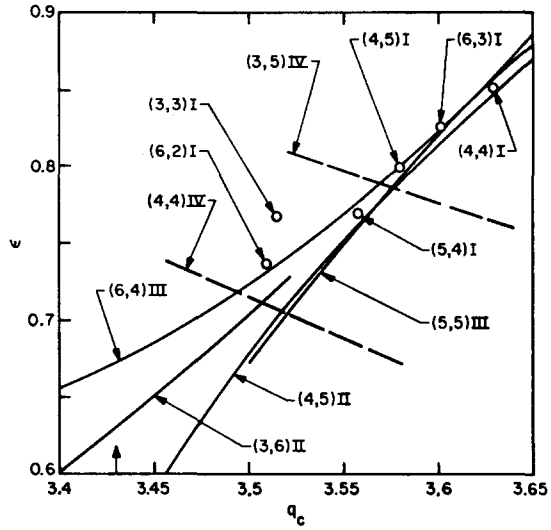

FIG. 9. Analysis of $g^{(4)}$. The indication of $q_c > 3.43$ is clear. Even the scatter in methods (ii) and (iii) is unusually large at the low end.

of determining α from series calculations are again illustrated.

G. Hypersusceptibility (Pressure Variable)

$$g^{(4)}(q)/kT \equiv (\partial^4 g/\partial y^4)_q\,|_{y=0}/kT = 2.0 - 0.75q^2 + 0.70312q^3 - 0.60066q^4 + 0.50282q^5 - 0.41864q^6 + 0.34794q^7 - 0.28913q^8 + 0.24034q^9 - 0.19991q^{10} + \cdots. \quad (4.7)$$

In Fig. 9 most of the relevant features of the Padé study of $g^{(4)}$ are revealed. The general trend of the data indicates a q_c somewhat higher than 3.430. If this is interpreted as merely indicative of slow convergence and the singularity is forced to agree with that of the susceptibility, one estimates $\epsilon = 0.65 \pm 0.1$. This is low compared with $\epsilon_\rho/(1-\alpha_\rho) = 0.71$.

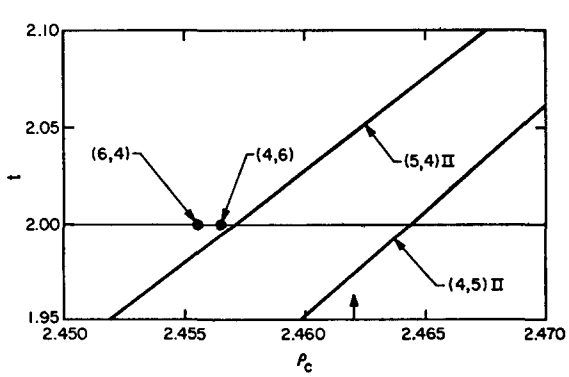

FIG. 10. Analysis of $K/\chi^2 f^{(4)}$. The filled circles indicate values of ρ_c determined from Padé approximants to $w^{1/2}$, hence are method (iii) points.

This article is copyrighted as indicated in the article. Reuse of AIP content is subject to the terms at: http://scitation.aip.org/termsconditions. Downloaded to IP: 128.112.66.66 On: Sun, 29 Dec 2013 03:06:19

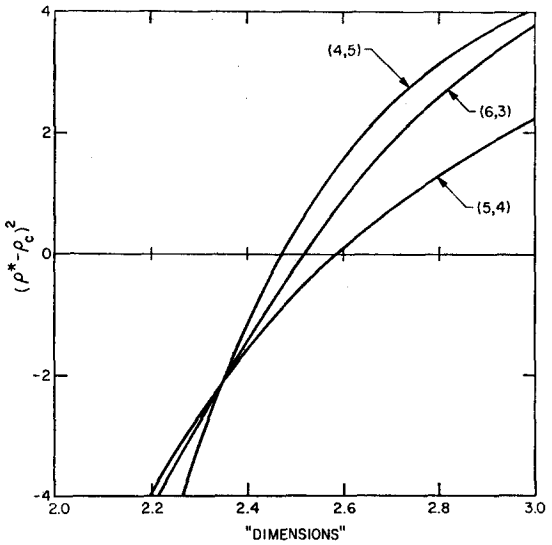

FIG. 11. Square of the difference between the two poles of $d\log\chi/d\rho$ on or near the positive real axis, as a function of "dimensionality." There is no critical singularity below about 2.5 dimensions.

H. The Scaling Law

The scaling-law relation $t\equiv 2\gamma_\rho+\alpha_\rho-\epsilon_\rho=2$ can be tested in two ways. Taking our estimates of γ_ρ, α_ρ, and ϵ_ρ we find $t\approx 2.04$. On the other hand one can determine the series of $w(\rho)=K/\chi^2 f^{(4)}$ [which should behave like $(\rho_c-\rho)^2$] and subject it to a Padé analysis. Results are shown in Fig. 10. The prediction is not very sharp, probably owing to the incorporation of the hypersusceptibility. For $\rho_c=2.463$ it appears that t is about 2.0.

It should be mentioned that method (i) applied to $w(\rho)$ yields much higher values of ρ_c and of t; viz., t in the range 2.3–2.7.

V. THE EFFECT OF VARYING DIMENSIONALITY

The free-energy function for any dimensionality is easily calculated once the determinants D_G are known. In fact, Eq. (3.1) even suggests a natural (though nonunique) way of associating a free-energy series with nonintegral dimensions. We have studied a number of the properties of the critical point as a function of the continuous dimensionality parameter d. The qualitative nature of the results can be understood by reference to Fig. 4 which illustrated the location of the singularities of $d\log\chi(\rho)/d\rho$. As the dimensionality d is increased from three the location of the phase-transition pole moves a bit toward the origin and the other poles move outward. (Beyond four dimensions erratic features appear in certain Padés.) For d smaller than 3 the two poles on the positive, real axis move together and eventually merge at about 2.5 "dimensions." For even lower dimensionality than 2.5, these poles split into a complex pair, so that the susceptibility is free of singularities on the real density axis. In Fig. 11 is plotted the square of the difference in location of these two poles as a function of dimensionality for several approximants to $d\log\chi/d\rho$. After the pair splits off the real axis the difference is imaginary, so the square is negative.

As a function of dimensionality, γ goes to unity for increasing dimensions, and goes to infinity as the system approaches the critical dimensionality at which the transition disappears.

Qualitatively the same features appear for the hypersusceptibility. It is impossible at present to answer the question of whether a transition in the hypersusceptibility remains for dimensionality less than 2.5 (higher-order phase transition).

The scaling law, $t\equiv 2\gamma_\rho+\alpha_\rho-\epsilon_\rho=2$ (independent of dimension) has also been tested for varying dimensions by studying the logarithmic derivative of $K/\chi^2 f^{(4)}$. In three dimensions t appeared to be only slightly above the scaling-law value of 2. For increasing dimensionality t falls and appears to continue to fall even slightly below two after four dimensions. For decreasing dimensions t rises. Although the uncertainties also increase, t appears to be greater than 2.4 for dimensionality equal to 2.5 [by method (ii)]. It is possible however that ρ_c for this dimensionality is very poorly determined, and the scaling law holds.

VI. TEMPERATURE AS AN INDEPENDENT VARIABLE

The general procedure for conversion from pressure to temperature as an independent variable is related to a discussion given by Pippard for He λ-line phenomena.[9]

While the above calculations were all carried out at that temperature, T_G, for which the Mayer f function is a Gaussian, it is probable that the exponents are not functions of the temperature at least for some finite interval around T_G. Thus one may extrapolate to other temperatures by replacing $p_c(T_G)-p$ by $p_c(T)-p_c$ Alternatively one can fix the pressure at a value which is critical for a temperature T_c, $p_c(T_c)$. Then one should have

$$p_c(T)-p_c(T_c)=(T-T_c)[\partial p_c(T_c)/\partial T]+\cdots. \quad (6.1)$$

If $\partial p_c/\partial T$ is positive and finite one can replace $p-p_c$ by $c(T-T_c)$ in all the formulas, including the scaling law form of the free energy, Eq. (2.7). One concludes that as one approaches the critical point at fixed pressure

$$\chi(T,p)\propto[T-T_c(p)]^{-\gamma}, \quad (6.2)$$

$$K(T,p)\propto[T-T_c(p)]^{-\alpha}, \quad (6.3)$$

etc. Furthermore, α is identical with the exponent characterizing the specific-heat singularity

$$c_p(T,p)\propto[T-T_c(p)]^{-\alpha}. \quad (6.4)$$

[9] A. B. Pippard, *Elements of Classical Thermodynamics* (Cambridge University Press, Cambridge, England, 1957).

This article is copyrighted as indicated in the article. Reuse of AIP content is subject to the terms at: http://scitation.aip.org/termsconditions. Downloaded to IP: 128.112.66.66 On: Sun, 29 Dec 2013 03:06:19

If it should be advisable to regard these thermodynamic variables as functions of density, rather than pressure, then the singularities corresponding to χ, κ, and c_p would be characterized by the exponents $-\gamma_\rho$, α_ρ, and α_ρ, respectively. As an example one has

$$K(T,\rho) \propto [T-T_c(\rho)]^{\alpha_\rho}. \tag{6.5}$$

The specific heat c_v for $y=0$ does not go to infinity at T_c but does have a cusp as a function of temperature at fixed density (recall α_ρ is negative)

$$c_v(T,\rho) \approx c_{v0}(\rho) - b(\rho)[T-T_c(\rho)]^{-\alpha_\rho}, \qquad b(\rho) \geq 0. \tag{6.6}$$

This can be derived by performing a Legendre transformation on (definition of α, not a scaling law):

$$g(p, y=0) \sim g_N(p,0) + b_0(p_c-p)^{2-\alpha}. \tag{6.7}$$

VII. CONCLUSIONS

The critical separation properties of mixtures, or at least the idealized Gaussian mixture treated here, appear to follow the same pattern as has emerged in the study of critical transitions in the gas–liquid, magnetic, binary alloy, and other systems. The exponent $\gamma=1.23$ is close to that observed in other three dimensional systems. The value $\alpha \approx 0.24$ or 0.29 is considerably higher however. This results, according to scaling laws, in a value of β of ~ 0.25 which is somewhat lower than other systems.

It is very difficult to say, on the basis of the calculations performed so far, just how closely we have converged to the true exponents. It is possible that a large, fast computer could be used to add one more term to our starting virial series, but beyond this new techniques would be required.

The analysis in terms of density variables appears to be superior to the pressure variable study. The latter is plagued by singularities in the negative half-plane close to the origin. Furthermore, the susceptibility singularity is more clearly revealed than that of other thermodynamic functions.

ACKNOWLEDGMENTS

We wish to thank Mrs. B. Grant and Mr. R. B. Kornegay for their skillful programming of the diagram generation scheme, and Mrs. Z. Wasserman for performing the Padé analyses. We are grateful to Dr. G. A. Baker, Jr. for providing us with his program for Padé approximant calculations and to Professor B. Widom for valuable comments.

APPENDIX A

The primary objective of this paper is the determination of critical region behavior for the binary Gaussian mixture bulk thermodynamic properties. In this Appendix we point out that certain inferences may be drawn from these bulk properties as to the character of molecular pair correlation functions for the model.

In view of the fundamental symmetry of our mixture model, there are but two independent pair correlation functions[10]:

$$g_{AA}^{(2)}(r) \equiv g_{BB}^{(2)}(r) \quad \text{and} \quad g_{AB}^{(2)}(r) \equiv g_{BA}^{(2)}(r). \tag{A1}$$

The relevant connection between these correlation functions and bulk solution properties is conveniently provided by the general Kirkwood–Buff solution theory.[11] At the critical composition $y=0$ one obtains the following identities:

$$\frac{2}{kT}\left(\frac{\partial^2 g}{\partial y^2}\right)_{p,T} = \frac{1+\rho(G_{AA}+G_{AB})}{1+\rho G_{AA}+(\rho^2/4)(G_{AA}^2-G_{AB}^2)}; \tag{A2}$$

$$\frac{1}{kT}\left(\frac{\partial \rho}{\partial p}\right)_{y,T} = \frac{1+(\rho/2)(G_{AA}-G_{AB})}{1+\rho G_{AA}+(\rho^2/4)(G_{AA}^2-G_{AB}^2)}; \tag{A3}$$

the quantities G_{AA} and G_{AB} are pair correlation-function spatial integrals,

$$G_{\alpha\beta} = \int [g_{\alpha\beta}^{(2)}(r) - 1]\,d\mathbf{r}. \tag{A4}$$

As the homogeneous binary mixture is isothermally compressed toward p_c, the impending phase separation is anticipated by local segregation of A and B molecules into patches or regions of irregular size and shape. The mean linear dimension of these critical clusters, however, does increase indefinitely as p increases to p_c. The correlation function $g_{AA}^{(2)}(r)$ manifests this clustering tendency of A around A and B around B by deviating positively from unity for larger and larger r as the transition is approached. Conversely, $g_{AB}^{(2)}(r)$ will deviate negatively from unity over a comparable range.

The increasing range of clustering in approach to the critical point implies the divergence of integrals G_{AA} and G_{AB}. We represent the most singular parts of these quantities in the critical region at $y=0$ in the following way ($p<p_c$):

$$G_{AA} \sim K(p_c-p)^{-\zeta},$$
$$G_{AB} \sim -K^*(p_c-p)^{-\zeta^*}. \tag{A5}$$

Each of the quantities K, K^*, ζ, and ζ^* are positive constants.

Three cases may now be distinguished:

Case I: $\zeta^* > \zeta$,

Case II: $\zeta^* = \zeta$,

Case III: $\zeta^* < \zeta$.

By using the expressions shown in Eq. (A5), the asymptotic behavior of thermodynamic quantities (A2) and (A3) may be deduced for each of the three cases:

[10] T. L. Hill, *Statistical Mechanics* (McGraw-Hill Book Co., New York, 1956), Chap. 6.

[11] J. G. Kirkwood and F. P. Buff, J. Chem. Phys. 19, 774 (1951).

This article is copyrighted as indicated in the article. Reuse of AIP content is subject to the terms at: http://scitation.aip.org/termsconditions. Downloaded to IP: 128.112.66.66 On: Sun, 29 Dec 2013 03:06:19

Case I

$$(2/kT)(\partial^2 g/\partial y^2)_{p,T} \sim (4/\rho_c K^*)(p_c - p)^{\zeta^*},$$

$$(1/kT)(\partial p/\partial \rho)_{y,T} \sim -(2/\rho_c K^*)(p_c - p)^{\zeta^*}; \quad \text{(A6)}$$

Case II

$$(2/kT)(\partial^2 g/\partial y^2)_{p,T} \sim [4/\rho_c(K+K^*)](p_c - p)^{\zeta},$$

$$(1/kT)(\partial p/\partial \rho)_{y,T} \sim [2/\rho_c(K-K^*)](p_c - p)^{\zeta}; \quad \text{(A7)}$$

Case III

$$(2/kT)(\partial^2 g/\partial y^2)_{p,T} \sim (4/\rho_c K)(p_c - p)^{\zeta},$$

$$(1/kT)(\partial p/\partial \rho)_{y,T} \sim (2/\rho_c K)(p_c - p)^{\zeta}. \quad \text{(A8)}$$

The second Case II expression tentatively assumes $K \neq K^*$.

We may immediately discard Case I, on account of the thermodynamic impossibility of negative compressibility.

Since we have concluded in Sec. IV that quantity (A2) vanishes more strongly at the critical point than quantity (A3), it is also necessary to discard Case III and the tentative-condition Case II as well. The only remaining option therefore is the special Case II situation, with both $K = K^*$ and $\zeta = \zeta^*$. Then, aside from a sign change, the critical singularities of G_{AA} and G_{AB} are identical in leading order. Unquestionably this implies that $g_{AA}^{(2)}(r)$ and $g_{AB}^{(2)}(r)$ deviate from unity at large r by equal and opposite amounts in the critical region.

The sum

$$\Gamma(p_c - p) = G_{AA} + G_{AB} = \int [g_{AA}^{(2)}(r) + g_{AB}^{(2)}(r) - 2]\,d\mathbf{r} \quad \text{(A9)}$$

measures the local increment in material density, regardless of species, around a central A (or B) molecule. Although the longest-ranged fluctuations of $g_{AA}^{(2)}(r)$ and $g_{AB}^{(2)}(r)$ from unity cancel one another, we must still anticipate that Γ might display a weak divergence at p_c as a result of only partial cancellation over still a rather long range in r.

In place of (A7) we now find

$$(2/kT)(\partial^2 g/\partial y^2)_{p,T} \sim (2/\rho_c K)(p_c - p)^{\zeta},$$

$$(1/kT)(\partial p/\partial \rho)_{y,T} \sim [1 + (\tfrac{1}{2}\rho_c)\Gamma(p_c - p)]^{-1}. \quad \text{(A10)}$$

The results of Sec. IV imply that ζ is identical with exponent γ. Furthermore we see that $\Gamma(p_c - p)$ must indeed diverge to infinity as

$$\Gamma(p_c - p) \sim \Gamma_0 (p_c - p)^{-\alpha}, \quad \text{(A11)}$$

where Γ_0 is a suitable positive constant.

One must conclude from (A11) that at least for the binary Gaussian mixture, the critical region manifests very large *total* density fluctuations, as well as the well-known *relative* density fluctuations. We suspect that this feature transcends the special model investigated in this paper; for general nonsymmetric continuum models of binary solutions it is likely that the matrix of quadratic composition and total density fluctuations develops two infinite eigenvalues at the critical point. This is in distinct contrast to the single infinite eigenvalue predicted by the classical solution theories.

APPENDIX B: GENERATION OF THE GRAPHS

The vertices of the Mayer graphs for mixtures are labeled A and B. The bicolored graphs are those with no bonds between two A points or two B points. They are easily drawn by placing the A and the B points in separate columns. The only allowed bonds are those going from one column to the other.

The bicolored graphs of n_A A points, n_B B points, and b bonds are obtained from those with $b+1$ bonds by striking out one bond. The graphs are examined by computer for multiple connectivity by tracing out paths between each pair of points.

Simple measures, based on classifying the points by the number of bonds entering them, avoid some duplications, but no algorithm exists to totally avoid repeats. Thus the diagrams must be compared for equivalence. Each diagram is denoted by a binary number (cf. Ref. 1). All the equivalent binary representations of one of the graphs are generated and arranged in numerical order (for ease of searching). The number of representations thus obtained is also needed in the Mayer series since it provides the required graph symmetry number. The remaining graphs generated by the striking out process are compared with this list and equivalent ones are removed. Then the rearranging and comparison is repeated with the next remaining diagram.

The determinant for each graph is evaluated using a theorem for partitioned determinants.[12]

The number of nonequivalent graphs of the various types is listed in Table II. The graphs required about an hour for generation on a GE 635, and the determinants took 0.06 h.

[12] R. Bellman, *Introduction to Matrix Analysis* (McGraw-Hill Book Co., New York, 1960), p. 103.

This article is copyrighted as indicated in the article. Reuse of AIP content is subject to the terms at: http://scitation.aip.org/termsconditions. Downloaded to IP: 128.112.66.66 On: Sun, 29 Dec 2013 03:06:19